nonlinear. If it is represented by a straight line of the form of Eq. 12, the equilibrium constant, K_e, is of the order of 100. The experimental D_p lies therefore in the expected range.

CONCLUSIONS

The Thomas model for fixed bed adsorption successfully correlates experimental data for the NH_3-Cu(II)-carboxylic acid resin ligand exchange system. Mass transfer parameters in the model lie in the expected ranges. The resin phase diffusivity calculated from one experimental run was used successfully to predict the breakthrough curve for a second run with different feed rate and feed concentration. The model should be useful for design and operation of ligand exchange columns.

NOTATION

a = surface area of resin pellets per unit volume of bed, cm^2/cm^3
b = correction factor for nonlinear equilibrium line
c = concentration of NH_3 in liquid phase, mol/cm^3
C_o = feed concentration, mol/cm^3
D_p = resin phase effective diffusivity, cm^2/s
D_e = ammonia diffusivity in resin pores
k = reaction rate constant
k_f = liquid phase mass transfer coefficient, cm/s
k_p = resin phase mass transfer coefficient, cm/s
K = equilibrium constant in Langmuir type isotherm
K_1,K_2,K_3 = formation constants for Cu(II)–NH_3 complexes
m = liquid phase molality, mol/kg water
M = resin phase molality, mol/kg water
n = dimensionless bed length
q = concentration of NH_3 in resin phase, mol/g
q_m = resin phase concentration in equilibrium with feed, mol/g
t = time, s
T = dimensionless time
v = velocity of fluid in void spaces of bed, cm/s
$v\epsilon$ = superficial velocity of fluid, cm/s
x = distance from bed inlet, cm
ϵ = void fraction for bed
ϵ_p = pellet void fraction
ρ_B = resin bulk density, g/cm^3
ρ_p = pellet density

LITERATURE CITED

Dawson, G. W., "Process for Removal of Ammonia from Aqueous Streams," U.S. 3,842,000 (1974).
Dobbs, R. A., S. Uchida, L. M. Smith, and J. M. Cohen, "Ammonia Removal from Waste Water by Liquid Exchange," *AIChE Symp. Ser.*, **71**, No. 152, p. 157 (1975).
Dobbs, R. A., "Ligand Exchange Process for Removal of Ammonia," U.S 3,948,769 (1976).
Helfferich, F., "Ligand Exchange. I: Equilibria," *JACS*, **84**, p. 3237 (1962a).
Helfferich, F., "Ligand Exchange. II: Separation of Ligands Having Different Coordinative Valences," *JACS*, **84**, p. 3242 (1962b).
Helfferich, F., *Ion Exchange*, McGraw-Hill Book Co., New York, p. 222. 445 (1962c).
Jeffrey, M., "Removal of Ammonia from Wastewater Using Ligand Exchange," M.S. Thesis, Louisiana State University (1977).
Sherwood, T. K., R. L. Pigford, and C. R. Wilke, *Mass Transfer*. McGraw-Hill, p. 579, 244 (1975).
Thomas, H. C., "Heterogeneous Ion Exchange in a Flowing System," *JACS*. **66**, p. 1664 (1944).
Yatsimirskii, K. B., and V. P. Vasiliev, *Instability Constants of Complex Compounds*, Van Nostrand, Princeton (1966).

Manuscript received June 16, 1982; revision received October 5, and accepted October 20, 1982.

Hydrodynamic Modelling for Liquid Holdups in Periodically Cycled Plate Columns

M. F. THOMPSON and I. A. FURZER

Department of Chemical Engineering
The University of Sydney
NSW 2006, Australia

The concept of periodic cycling of liquid and vapor streams in perforated plate columns was developed by Cannon (1961). Solution of the mass transfer equations by McWhirter and Lloyd (1963) showed a theoretical plate efficiency double that of a conventional column. Robertson and Engel (1967) found this efficiency was dependent on the fraction of the liquid holdup drained from the plate. Subsequent extensions to the theory by May and Horn (1968) and Furzer (1973) confirmed these findings.

In all these studies, prior knowledge of the liquid holdups in the column was necessary to solve the mass transfer equations. Horn (1967), Gerster and Scull (1970), and Furzer and Duffy (1976) presented experimentally-based mixing models to overcome this problem. However, no correlations between these models and the design parameters of a column were obtained.

Wade et al. (1969) investigated the liquid and vapor flows in a periodically-cycled column implementing two different sets of tray performance equations. Their simple hydrodynamic model was based on the difference between the wet plate pressure drop and the hydrostatic head, which dictated whether liquid or vapor flow occurred. The other model utilized the more complex analysis of tray behavior by Prince and Chan (1965) with simultaneous liquid and vapor flow.

Larsen and Kummel (1979) further developed the latter model, examining flow profiles in the column. Both groups of workers

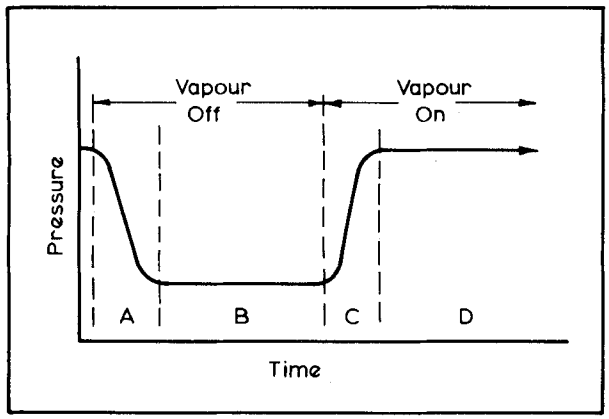

Figure 1. Idealized pressure response: region A & C = dynamic responses; B = liquid drain; D = steady-state vapor flow.

concluded a system to equalize column pressures at the beginning of the liquid flow period (LFP) was necessary. In neither case were the results of their simulations experimentally confirmed.

The use of a hydrodynamic model to predict the steady-state holdups in a periodically-cycled column has not been reported.

THEORY

A periodically-cycled column undergoes four modes of operation during each cycle. These can be characterized by the pressure response under a plate, Figure 1. It consists of two dynamic parts, A and C, resulting from the removal and introduction of the vapor supply, a liquid drain period, B and a steady-state vapor flow period D.

An air-water system, Figure 2, was studied. The column was fitted with a branch resistant manifold and Time Delay Plates, developed by Furzer (1980), to improve the hydrodynamic conditions.

The simple tray behavior model of Wade et al. (1969) was used to determine liquid and vapor velocities. The difference ΔP_n between wet plate pressure drop and the hydrostatic head dictated whether liquid or vapor flow occured.

$$\Delta P_n = P_n - P_{n-1} - \rho_L g h_n \tag{1}$$

Vapor velocities

$$V_{p,n} = \left(\frac{2\Delta P_n}{\rho_V k_{V,n}}\right)^{1/2} \qquad \Delta P_n \geq 0 \tag{2}$$

$$V_{p,n} = 0.0 \qquad \Delta P_n < 0$$

Liquid velocities

$$L_{p,n} = \left(\frac{-2\Delta P_n}{\rho_L k_{L,n}}\right)^{1/2} \qquad \Delta P_n < 0 \tag{3}$$

$$L_{p,n} = 0.0 \qquad \Delta P_n \geq 0$$

The manifold velocity $V_{m,n}$ is determined from an orifice equation.

$$V_{m,n} = \left[\frac{2(P_n - P_o)}{\rho_V k_{V,n}}\right]^{1/2} \tag{4}$$

The liquid velocity leaving the time delay downcomers $L_{d,n}$ depends on the velocity from the plate above and downcomer design parameters.

Liquid material balances were taken over the plate holdup, h_n, and the delayed liquid volume in the downcomer, M_n.

$$\frac{dh_n}{dt} = \beta(L_{d,n-1} - L_{p,n}) \tag{5}$$

$$\frac{dM_n}{dt} = A_c\beta(L_{p,n} - L_{d,n}) \tag{6}$$

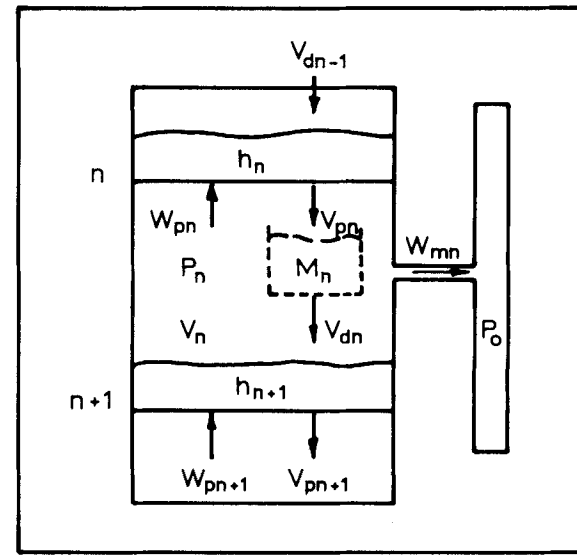

Figure 2. Liquid and vapor velocities for plate *n*.

where the liquid velocities, L, are based on the column free area, β.

A vapor material balance on volume G_n

$$\frac{dm_n}{dt} = \rho_V A_c(V_{p,n+1} - V_{p,n}) - \rho_V A_m V_{m,n} \tag{7}$$

was combined with a differential ideal gas equation

$$\frac{dm_n}{dt} = \frac{MW}{RT}\left(P_n\frac{dG_n}{dt} + G_n\frac{dP_n}{dt}\right) \tag{8}$$

The vapor volume G_n is dependent on the delayed liquid volume in the downcomer and the plate holdup.

$$\frac{dG_n}{dt} = -A_c\frac{dh_{n+1}}{dt} - \frac{dM_n}{dt} \tag{9}$$

The pressure response of the system is thus described by

$$\frac{dp_n}{dt} = \frac{\rho_V\frac{RT}{MW}(A_c(V_{p,n+1} - V_{p,n}) - A_m V_{m,n}) + P_n\left(A_c\frac{dh_{n+1}}{dt} + \frac{dM_n}{dt}\right)}{(A_c(H_n - h_{n+1}) - M_n)} \quad \text{for } n = 1, \ldots N \tag{10}$$

SOLUTION METHODS

For a column with N plates, there are $3N$ differential equations. Three variable step size solution techniques were employed to solve the equations for a four-plate column. They were the Runge-Kutta-Merson (RKM) method, the predictor-corrector Adams procedure and the Gear method for stiff differential equations with internal Jacobian evaluation. The routines were obtained from the NAG (1978) algorithm library and run on a CYBER 170-173.

The integrations commenced at the beginning of the LFP and were performed until steady state was achieved within the cycle. Intermediate output was interpolated internally by the routines at specified intervals.

The physical parameters were set according to the experimental air-water system with a cycle time of 20.0 s, a LFP of 2.0 s, and an instantaneous valve response. The pressures were scaled in kPa and the local error bound set to 10^{-5}.

The relative computing times and typical holdup responses are presented in Figures 3 and 4. The effects of the local error tolerance

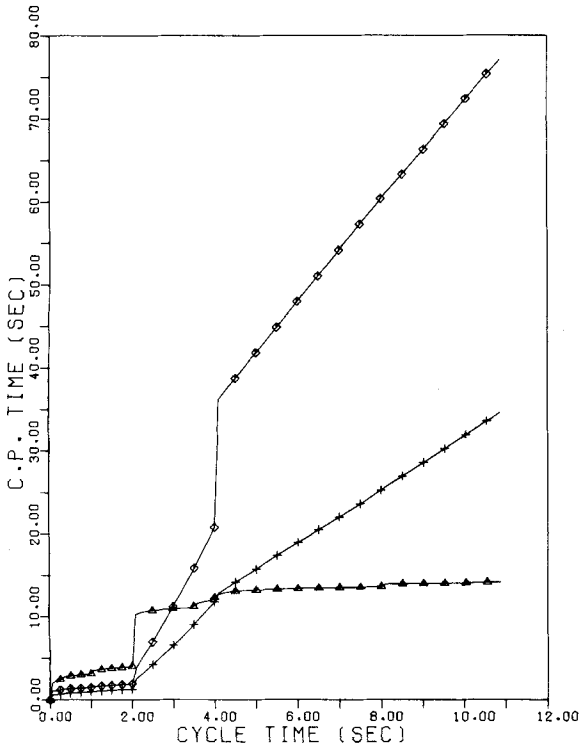

Figure 3. Comparative computing times required as a function of elapsed cycle time: △ Gear; + Runge-Kutta-Merson; ◇ Adams.

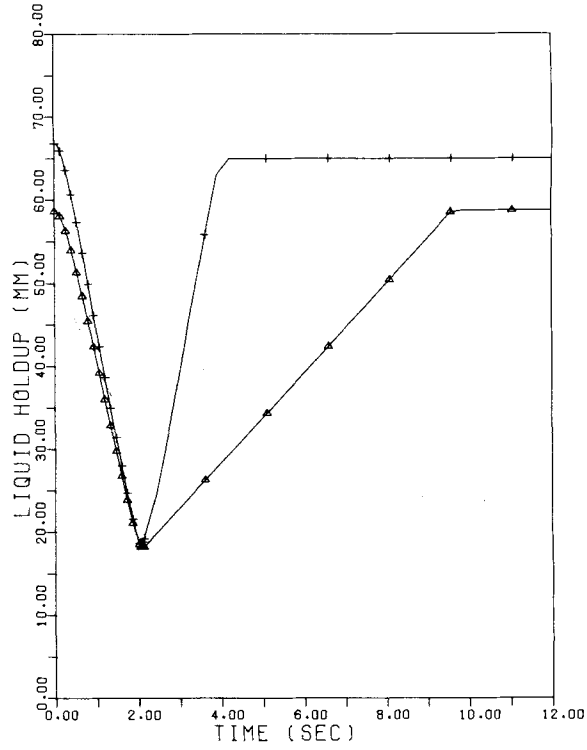

Figure 4. Liquid holdup response: Drain time 2.0 s △ Plate 1; + Plate 4.

on the holdup global error and computing time required to attain steady-state conditions are shown in Table 1.

The accuracy was estimated by comparison with the solution at a local error tolerance of 10^{-8}. The global errors for the RKM method were confirmed by a NAG (1978) routine using the technique of Shampine and Watts (1976).

EXPERIMENTAL

A 600 mm diameter perspex column containing four sieve plates with 6% free area and 6 mm holes was supplied with metered air from a 20 kW fan.

The air supply and liquid feed were controlled in an on/off mode with solenoid actuators operated by a dedicated MOS Technology 6502 microprocessor. The system is as described by Furzer and Rosolen (1978).

The column was fitted with Time Delay Plates to improve plug flow characteristics and a 25 mm diameter branch resistance manifold to assist pressure equilization at the start of the LFP. The branches below plates 1 to 3 were fitted with 8 mm diameter restrictions.

The dynamic pressure responses under each plate were followed by National Semiconductor Differential Pressure Transducers LX1701DD and logged by a PDP 11/45 with real time data acquisition facilities at 30 readings a second. A typical series of response curves are shown in Figure 5.

TABLE 1 SOLUTION ACCURACY AND REQUIRED COMPUTING TIME TO REACH STEADY STATE WITHIN CYCLE.

Method	Tolerance	Accuracy	CPU Time (s)
Gear	10^{-3}	4×10^{-5}	7.0
	10^{-4}	5×10^{-6}	10.29
	10^{-5}	1×10^{-6}	14.06
RKM	10^{-3}	1×10^{-6}	31.14
	10^{-4}	1×10^{-7}	31.53
	10^{-5}	1×10^{-7}	31.89
Adams	10^{-3}	7×10^{-5}	58.19
	10^{-4}	1×10^{-5}	59.72
	10^{-5}	2×10^{-7}	72.20

Model and experimental data comparisons for the pressures below plates 1 and 3 are presented in Figure 6 with plates 2 and 5 in Figure 7.

DISCUSSION

The solution of the mass transfer equations for a periodically cycled column requires details of the plate holdups. At present, these can only be determined experimentally. The ultimate ob-

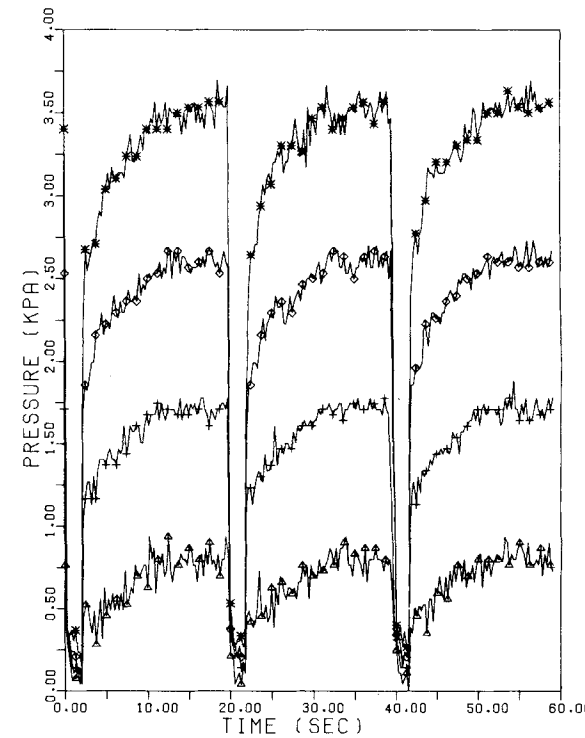

Figure 5. Typical pressure response curves from experimental air-water system: △ Plate 1; + Plate 2; ◇ Plate 3; * Plate 4.

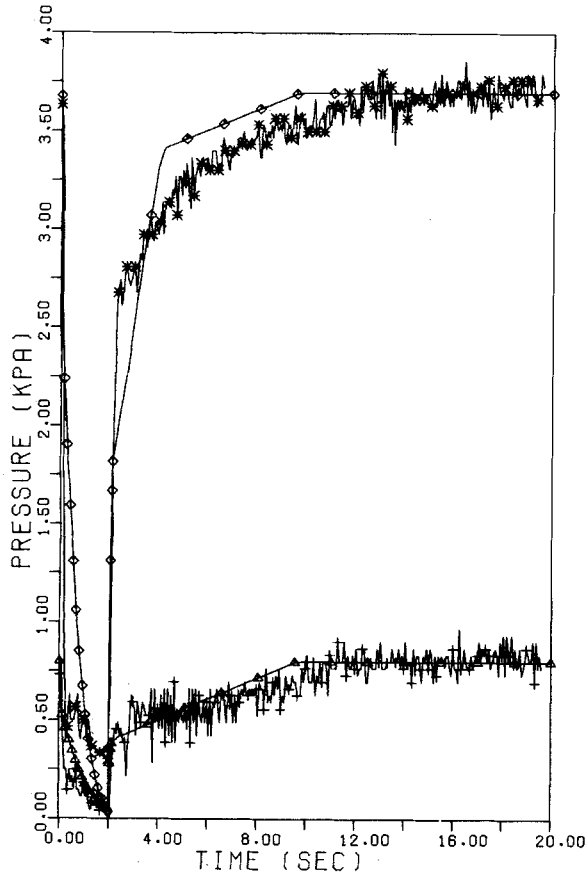

Figure 6. Comparison of model with experimental pressure response: Plates 1 and 3. Cycle time, 20.0 s; drain time, 2.0 s; experimental response = △ Plate 1, ◇ Plate 3; model response = + Plate 1, * Plate 3.

jective of the hydrodynamic model is to predict the holdup distribution in a periodically-cycled column, for a specific set of design and operating conditions.

The performance of the hydrodynamic model in describing the column behavior, was initially investigated by comparison of the pressure responses, over a single cycle. Once the validity of the dynamic model has been confirmed, the plate holdups can be obtained from a minimization of the sum of squares differences between comparable points in the steady-state vapor flow period (VFP).

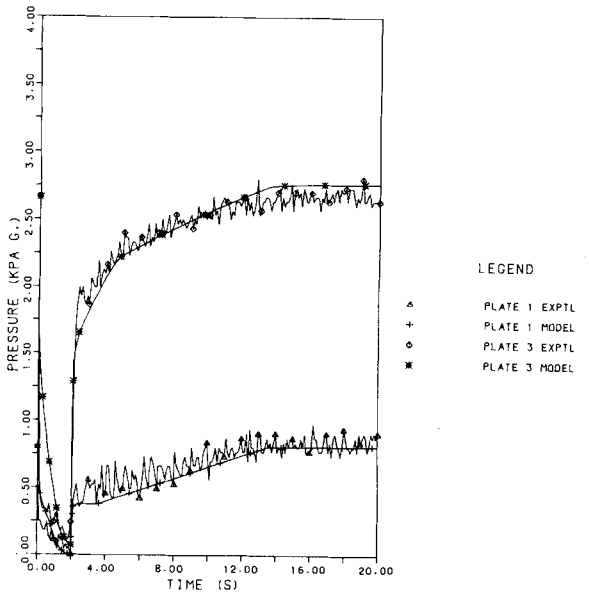

Figure 7. Comparison of model with experimental pressure response: Plates 2 and 4. Cycle time, 20.0 s; drain time, 2.0 s; experimental response = △ Plate 2; ◇ Plate 4; model response = + Plate 2; * Plate 4.

The results presented in Figures 6 and 7 show a favorable comparison between the experimental and model responses during the VFP. The greatest deviations occurred in the dynamic regions of the cycle. These differences result from using a simple on/off model to represent the air supply system. The fan was operated with a head in excess of 3 kPag. during the VFP, reducing to virtually zero when the air was bypassed from the column. A more detailed model to compensate for these dynamics would not improve the simulation in the region of interest.

Determination of the steady-state plate holdups by minimization of the sum of squares requires an efficient solution method for the dynamic equations. The results in Figure 3 and Table 1 show that the RKM technique is best suited for the LFP, where all derivatives are of a similar magnitude. After the initial dynamics of the VFP, the equations become stiff with changes in the holdups resulting in comparatively smaller pressure increases. The best strategy involves a switch from the RKM to the Gear method, in the early stages of the VFP.

The results of the dynamic studies show the simple hydrodynamic model constitutes a satisfactory basis for the estimation of holdups in a periodically-cycled distillation column.

NOTATION

A = area, m^2
g = acceleration due to gravity, m/s^2
G = vapor volume, m^3
h = liquid holdup on plate, m
H = plate spacing, m
k = resistance to fluid flow
L = liquid velocity, m/s
m = mass of vapor, kg
M = delayed volume of liquid in downcomer, m^3
MW = molecular weight of vapor, kg/kmol
P = pressure, kPa
R = gas constant, J/K·kmol
t = time, s
T = vapor temperature, K
V = vapor velocity, m/s

Greek Letters

β = plate free area
ρ = vapor density, kg/m^3

Subscripts

c = column
d = delayed
L = liquid
m = manifold
n = plate number
p = plate
V = vapor

LITERATURE CITED

Cannon, M. R., "Controlled Cycling Improves Various Processes," *Ind. Eng. Chem.*, **53**, No. 8, p. 629 (1961).

Furzer, I. A., "Periodic Cycling of Plate Columns," *Chem. Eng. Sci.*, **28**, p. 296 (1973).

Furzer, I. A., and C. J. Duffy, "Periodic Cycling of Plate Columns: Discrete Residence Time Distribution," *AIChE J.*, **22**, No. 6, p. 1118 (1976).

Furzer, I. A., and K. R. Rosolen, "Microprocessor System for Plate Column Control," *IEEE Trans. IECI*, **25**, No. 2, p. 145 (1978).

Furzer, I. A., Australian Patent App. 58743/80 (1981).

Gerster, J. A., and H. M. Scull, "Performance of Tray Columns Operated in the Cycling Mode," *AIChE J.*, **16**, No. 1, p. 108 (1970).

Horn, F. J. M., "Periodic Countercurrent Processes," *Ind. Eng. Chem. Process Design Dev.*, **6**, No. 1, p. 30 (1967).
Larsen, J., and M. Kümmel, "Hydrodynamic Model For Controlled Cycling in Tray Columns," **34**, No. 4, p. 455 (1979).
McWhirler, J. R., and W. A. Lloyd, "Controlled Cycling in Distillation and Extraction," *Chem. Eng. Prog.*, **59**, No. 6, p. 58 (1963).
May, R. A., and F. J. M. Horn, "Stage Efficiency of a Periodically Operated Distillation Column," *Ind. Eng. Chem. Process Design Dev.*, **7**, No. 1, p. 61 (1981).
NAG, "Fortran Library Manual, Mark 8," Numerical Algorithm Group (1981).
Prince, R. G. H., and B. K. C. Chan, "The Seal Point of Perforated Distillation Plates," *Trans. Inst. Chem. Engrs.*, **43**, p. T49 (1965).
Robinson, R. G., and A. J. Engel, "An Analysis of Controlled Cycling Mass Transfer Operations," *Ind. Eng. Chem.*, **59**, No. 3, p. 22 (1967).
Shampine, L. F., and H. A. Watts, "Global Error Estimation for Ordinary Differential Equations," *ACM Trans. Math. Software*, **2**, p. 172 (1976).
Wade, H. L., C. H. Jones, T. B. Rooney, and L. B. Evans, "Cyclic Distillation Control," *Chem. Eng. Prog.*, **65**, No. 3, p. 40 (1969).

Manuscript received March 29, 1982; revision received August 2, and accepted August 30, 1982.

Gas-Particle Mass Transfer in Trickle Beds

PAN ZHENG LU and J. M. SMITH
University of California
Davis, CA 95616

and

MORDECHAY HERSKOWITZ
Ben Gurion University of the Negev
Beer Sheva, Israel

At relatively low rates in trickle-bed reactors, flowing liquid appears not to cover the entire outer surface of the catalyst particles (Satterfield, 1975, Herskowitz et al., 1979). Under these conditions mass transfer from gas-to-particle as well as from gas-to-liquid and liquid-to-particle can influence reactor performance (when there is a limiting gaseous reactant). Mass transport from liquid to particle has been studied, for example by Goto et al. (1975), and from gas to liquid by Reiss (1967), Gianetto et al. (1973), and others. However, no information seems to be available for mass transfer coefficients k_{gs} from gas to the so-called gas-covered surface, that is, the particle surface not covered by flowing liquid. For catalysts of moderate or low activity and for slightly soluble gaseous reactants, the concentrations of reactant in the gas and on the gas-covered surface are nearly in equilibrium with each other. Thus, Herskowitz et al. (1979) found no effect of gas flow rate for the hydrogenation of α-methyl styrene using a Pd/Al_2O_3 catalyst of moderate activity. Hence, equilibrium could be safely assumed at the gas to gas-covered surface. With a more active catalyst for the same reaction, Herskowitz and Mosseri (1981) observed a significant change in global rate of reaction with gas flow rate, suggesting that gas-to-particle transport retarded the rate.

It is difficult to conceive of a reliable, direct method of measuring k_{gs}. However, the rate data of Herskowitz and Mosseri, along with available correlations for liquid-to-particle mass transfer coefficients, k_{LS}, can be used for an indirect evaluation of k_{gs}. We present here values of k_{gs} for trickle beds determined in this way. The method is suitable when the global rate is observed to vary with gas velocity.

In the Herskowitz and Mosseri study a differential reactor was used and the gas and liquid feed streams were in equilibrium with respect to hydrogen concentration. Hence, gas-to-liquid-to-particle mass transfer could be expressed in terms of a mass-transfer coefficient k_{Ls} from liquid to particle. For these conditions, and assuming the weighting factor model, Tan and Smith (1980) developed a relationship between the overall effectiveness factor η_o (a measure of the global reaction rate), the fraction f of the particle surface covered by flowing liquid, and the two mass transfer coefficients k_{gs} and k_{Ls}. Solved for k_{gs} this relationship is

$$Nu_{gs} = \frac{\epsilon_p k_{gs} H r}{D_e} = \frac{\phi_s \left[\frac{1}{\tanh\phi_s} - \frac{1}{\phi_s}\right]}{\left[\eta_o - \frac{f\left(\frac{C_L^b}{C_L^*}\right)\frac{3}{\phi_s}\left(\frac{1}{\tanh\phi_s} - \frac{1}{\phi_s}\right)}{1 + \frac{\phi_s}{Nu_{Ls}}\left(\frac{1}{\tanh\phi_s} - \frac{1}{\phi_s}\right)}\right]^{-1} - (1-f)\frac{3}{\phi_s}\left(\frac{1}{\tanh\phi_s} - \frac{1}{\phi_s}\right)} \tag{1}$$

where

$$Nu_{Ls} = \frac{\epsilon_p k_{Ls} r}{D_e} \tag{2}$$

$$\phi_s = r\left(\frac{k\rho_p}{D_e}\right)^{1/2} \tag{3}$$

The concentration ratio (C_L^b/C_L^*) is equal to unity for the differential reactor conditions employed, and k and D_e are known from the experimental data of Herskowitz and Mosseri, as is η_o. The surface coverage f was also calculated by these authors from an equation like Eq. 1 but based upon negligible mass transfer resistance from gas to particle; that is, taking $Nu_{gs} = \infty$. Such f values will be correct only for a gas flow rate equal to infinity. Hence, the f results of Herskowitz and Mosseri are first extrapolated to an infinite velocity as shown in Figure 1.

The only remaining unknown in Eq. 1 is Nu_{Ls}, and this can be estimated from the correlation of Goto et al. (1975). The results for k_{gs} calculated in this way are given in Figure 2 for various liquid